Volume and Multi-Slice Localizations Using Spatial-Spectral Selective RF Pulses for Selective Multiple-Quantum (Sel-MQC) Spectroscopic Imaging of Human Breast Cancer

Q. He[1,2], X. J. Zhou[3,4]

[1]MR Research Center, Radiology and Bioengineering, University of Pittsburgh, Pittsburgh, PA, United States, [2]University of Pittsburgh Cancer Institute, University of Pittsburgh, Pittsburgh, PA, United States, [3]Neurosurgery and Bioengineering, University of Illinois Medical Center, Chicargo, IL, United States, [4]Center for MR Research, University of Illinois Medical Center, Chicago, IL, United States

INTRODUCTION. In most extracranial organs, tissue ^{1}H NMR spectra are dominated by intense water and lipid resonances that block observation of metabolites and drugs. The human breast tissues represent perhaps the worst-case scenario for ^{1}H MRS due to the abundant lipids.[1] *In vivo* clinical observation of lactate, for example, has been challenging in breast and other extracranial cancers, although Roebuck *et. al.* have applied ^{1}H MRS to breast cancer for choline detection using spin-echo techniques.[2] To overcome these obstacles, we have developed the Selective Multiple-Quantum Coherence transfer (Sel-MQC) methods that completely suppress lipid and water in a single scan, for observing metabolites and antineoplastic agents in tissues containing high concentration of mobile fat.[3-6] These methods have been demonstrated for simultaneous lactate and choline detection in EMT6 tumors[4] and for Iproplatin detection in RIF-1 tumors.[5] The T_1- and T_2-Sel-MQC sequences were developed to determine relaxation times of the edited lactate signals for tissue metabolite quantification.[7] Modified Sel-MQC sequences are available to detect neuronal metabolites, such as glucose, GABA and glutamate with reduced signal overlap and excellent water suppression.[8, 9] Recently, we developed a multi-slice Sel-MQC method for 3D mapping of metabolites using the Hadamard matrix approach,[10] as well as the volume selective Sel-MQC techniques using 1331 composite pulses.[11] However, these methods are cumbersome to implement for clinical cancer studies and sometimes require high RF power that exceeds the hardware capability and SAR limitations of the clinical scanners. Here we report several Sel-MQC schemes using spatial-spectral (SPSP) selective RF pulses for volume or multi-slice localization. Overcoming the limitations of the previous Sel-MQC localization methods, the newly proposed techniques are easy to implement and permit interleaving 3D Sel-MQC imaging of metabolites in tissues containing high concentration of fat.

METHODS. *SPSP RF pulse design*. The magnetization profile in the spatial-spectral coordinates can be approximated by an inverse Fourier transformation of the function $B_1(t)/k'(t)$ defined along k-space sampling grid, where $k_z(t) = -\gamma\int_t^T G_z(s)ds$ is defined traditionally in the spatial dimension of k-space and $k_w(t) = t - T$ in the time dimension, $B_1(t)$ designates a shaped RF pulse and $k'(t)$ is a normalization factor of the sampling grid.[12] In this study, we designed two SPSP pulses using a Shinnar-Le Roux (SLR) algorithm [13]. The first pulse has a pulse width of 20ms while the second one 15ms. In both pulses, "true null" design[12] was used to eliminate the unwanted resonant peaks in the frequency domain. In this way, the pulse performance does not rely on signal cancellation of the magnetizations within the excited slice. To achieve a narrow spectral bandwidth without using excessively long pulse width, a small time-bandwidth product (~2) was employed in both pulse designs. Although this compromised the sharpness of the spectral profile, the resultant spectral response was adequate for the proposed applications. A simulation was performed by numerically solving the Bloch equations to evaluate the spatial and spectral selectivity of the pulses. The 20 ms pulse gave a pass-band spectral width of 100Hz as expected from the pulse design. The region without any excitation was 160 Hz away from the center of the pass-band. The side lobes on either edge of the spectral axis did not cause substantial perturbation to the magnetization, especially at the center of the slice. The response of the spatial domain was clean with negligible ripples. On the GE 3T scanner equipped with a CRM gradient, slice thickness as thin as 1mm can be achieved with the 20ms pulse.

Sel-MQC. In the Sel-MQC CSI pulse sequence, $90^0_\phi(C\underline{H}_3, lipid)$ -1/2J- $90^0_x(C\underline{H}, \underline{H}_2O)$ -t_1/2,g_1- $180^0_x(C\underline{H}_3, lipid)$ - $t_1/2, g_2$ - $90^0_x(C\underline{H}, \underline{H}_2O)$ - $g_3, \tau \pm t_1$ - acq, only lactate was excited into the MQ-states by the 20 ms SPSP 90^0 pulses. The signals of lipid and water remaining in the SQ modes were completely suppressed by the MQC-selection gradient pulses (g_1: g_2: g_3 =0:-1:2 or 1:0:2) (Fig. 1). Phase-encoding gradients were applied in two-dimensions defining the selected slice or volume.

RESULTS AND DISCUSSIONS. In the Sel-MQC sequence (Fig. 1a) we used a SPSP 90º pulse as the first RF pulse to map the cross section of a selected slice (Fig. 1b). When the spectral offset of the SPSP 90º RF pulse was set on water, instead of lactate CH_3, we could not detect the lactate signal, demonstrating the SPSP 90^0 pulse has excellent spectral selectivity. When the gradient pulse accompanying the SPSP 90º pulse was removed, the SPSP 90^0 pulse gave the similar spectral selectivity to a SINC pulse with a 100 Hz excitation band. The volume localization of SPSP-Sel-MQC was achieved by replacing all 90º pulses with the SPSP-90º pulses (Fig. 2a). Phase-encoding in the two orthogonal SPSP-pulse/gradient dimensions localized a plane, while the third direction of the volume was defined by the slice-selective SLR 180º pulse (the highest RF pulse in Fig. 2b). When applying all the SPSP-90° pulses and the slice-selective 180° pulse to define a slice in the same direction, we carried out the MQC transfer and lipid/water suppression in a single slice without affecting spins outside the slice of interest in the sample. This allows interleaved multi-slice localization of Sel-MQC CSI to be performed for human breast cancer studies within a desired 3D volume. This technique was implemented on the GE 3T scanner for clinical trials.

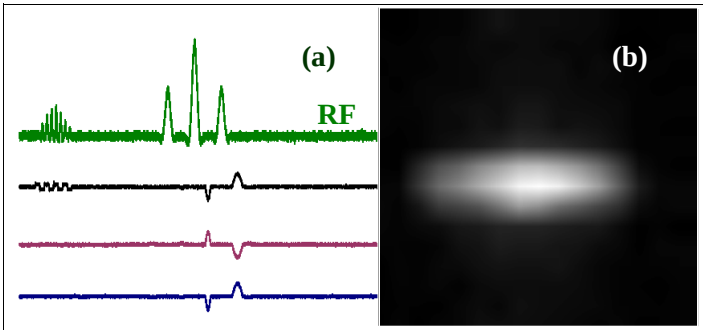

Fig. 1 The Sel-MQC sequence from oscilloscope with the first pulse being a SPSP 90º pulse for slice localization and frequency selective excitation. Phase encoding was applied to map the cross-section of the selected slice (b) from the GE Braino phantom on a GE 3T MRI scanner.

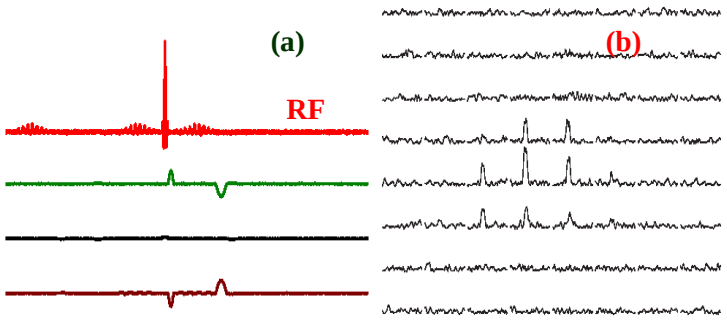

Fig. 2 The SPSP Sel-MQC sequence (a) for volume localization with phase-encoding in the 180° slice selective direction. (b) the lactate map with volume localization in the GE braino phantom on the GE 3T scanner.

CONCLUSIONS. We have demonstrated the principles to use SPSP selective RF pulses for volume and interleaved multi-slice localizations in the Sel-MQC experiments. The methods are easy to use on clinical MRI scanners, as in the PRESS and STEAM CSI techniques. Clinical breast cancer trials will soon be carried out upon approval by the IRB committee.

ACKNOWLEDGMENTS. The work was supported from Susan G. Komen Breast Cancer Foundation (Grant IMG0100117) and NIH (grant R21CA80906).

REFERENCES: 1. Sijens, P.E., *et al. Radiology* **169**, 615-20 (1988). 2. Roebuck, J.R., *et al Radiology* **209**, 269-275 (1998). 3. He, Q., *el al JMR. B* **106**, 203-211 (1995). 4. He, Q., *et al JMR, Series B* **112**, 18-25 (1996). 5. He, Q., *et al MRM* **33**, 414-416 (1994). 6. Bhujwalla, Z.M., *et al* in *NMR in Physiology and Biomedicine* (eds. Gillies, R.J.) 311-28 (Academic Press, San Diego, 1994). 7. Muruganandham, M., *et al MRM* **52**, 902-906 (2004). 8. De Graaf, R.A., *et al MRM* **43**, 621-6 (2000). 9. Shungu, D.C., *et al. Proc. ISMRM* **11**, 1140 (2003). 10. He, Q., *et al. Proc. ISMRM* **3**, 1447 (1997). 11. Thakur, S.B. & He, Q. *Proc. ISMRM* 1141 (2003). 12. Meyer, C.H., *et al MRM* **15**, 287-304 (1990). 13. Pauly, J.M., *et al IEEE Trans. Med. Imag.* **10**, 53-65 (1991).